Civil Engineering and Applied Solutions

Research Article

journal homepage: ceas.journals.umz.ac.ir

CEAS Civil Engineering and Applied Solutions

Data-Driven Prediction of FRP Confinement Efficiency in Concrete Columns: Incorporating Corner Radius and Aspect Ratio Effects

Sajjad Shayanfar [a], Meysam Ghasemi Naghibdehi [a], Javad Shayanfar [b*]

[a] *Department of Civil Engineering, Qaemshahr Branch, Islamic Azad University, Qaemshahr, Iran*
[b] *Department of Civil Engineering, University of Minho, Azurém, Guimarães 4800-058, Portugal*

ARTICLE INFO

Keywords:
FRP confinement
Compressive strength
Predictive model
Design-oriented model
Confined concrete
Non-circularity effect

Article history:
Received 10 December 2025
Accepted 29 January 2026
Available online 01 July 2026

ABSTRACT

This study develops a regression-based, design-oriented model for predicting the ultimate axial compressive strength of concrete columns fully confined with fiber-reinforced polymer (FRP) jackets. The model is formulated to be applicable to circular, square, and rectangular cross-sections within a single unified framework. Confinement effectiveness in non-circular sections is explicitly accounted for through two continuous geometric correction factors: one defined by the ratio of corner radius to section dimension and another defined by the cross-sectional aspect ratio. These factors modify the effective lateral confining pressure to reflect the progressive reduction in confinement efficiency as the section deviates from circularity. The model is calibrated and validated using a comprehensive experimental database comprising 1,723 FRP-confined concrete column tests, covering unconfined concrete compressive strengths from 6.6 to 204 MPa, FRP elastic moduli ranging from 13.6 to 657 GPa, and rectangular section aspect ratios up to 2.0. By construction, the formulation satisfies essential physical boundary conditions, including recovery of unconfined concrete strength in the absence of FRP confinement and a smooth, continuous transition in predicted strength between circular and non-circular cross-sections. The proposed model provides a general-purpose and physically consistent tool suitable for the design and assessment of FRP-confined concrete columns with varying cross-sectional geometries.

1. Introduction

The use of fiber-reinforced polymer (FRP) composites for externally confining reinforced concrete (RC) columns has become a well-established method for enhancing concrete's mechanical performance and the overall structural behavior of RC elements. Specifically, FRP confinement can substantially improve compressive strength, deformation capacity, and energy absorption, as well as increase load-carrying capacity, stiffness, and energy dissipation of columns [1-7]. Considerable research has focused on the axial stress-strain response of FRP-confined concrete, particularly for columns with non-circular cross sections (e.g., [8-11]). Experimentally observed axial stress-strain curves often exhibit a post-peak softening branch, reflecting strength reduction with increasing axial strain. Experimental studies indicate that this behavior is primarily influenced by several factors: (i) FRP confinement stiffness, (ii) the compressive strength of the concrete, (iii) non-circularity of the column cross-section, and (iv) the overall dimensions of the column [3, 12-18]. Eid et al. [19] performed axial compression tests on fully FRP-confined circular concrete columns (FFCC) with varying confinement stiffness. Their results show that high-stiffness FRP jackets effectively restrain lateral expansion, producing full strain-hardening behavior with substantial gains in axial strength and deformability. Conversely, reducing the confinement stiffness gradually shifts the response toward post-peak softening or softening–hardening behavior, with

* Corresponding author.
E-mail addresses: arch3d.ir@gmail.com (J. Shayanfar).

https://doi.org/10.22080/ceas.2026.30750.1059
ISSN: 3092-7749/
How to cite this article: Shayanfar, S., Ghasemi Naghibdehi, M., Shayanfar, J. Data-Driven Prediction of FRP Confinement Efficiency in Concrete Columns: Incorporating Corner Radius and Aspect Ratio Effects. Civil Engineering and Applied Solutions. 2026; 2(3): 1–15. doi:10.22080/ceas.2026.30750.1059.

the extent of this transformation directly linked to the FRP stiffness, as also noted by Wei and Wu [20]. Additionally, Fallah Pour et al. [21] and Vincent and Ozbakkaloglu [22] observed that the crack pattern evolves from diffuse microcracking to localized macrocracks as the behavior transitions from strain hardening to softening. Experimental studies by de Oliveira Diôgo et al. [23] show that the effectiveness of FRP confinement decreases as the concrete compressive strength increases. This reduction occurs because high-strength concrete exhibits lower lateral strain, delaying the activation of FRP confinement. Unlike normal-strength concrete (NSC), FRP-confined high-strength (HSC) or ultra-high-strength concrete (UHSC) columns often display post-peak strength loss beyond the transition zone, with the extent depending on the FRP stiffness. However, if sufficient lateral strain develops during softening, HSC/UHSC columns may undergo a strain-hardening phase due to the engagement of passive FRP confinement. This combined response, termed strain softening–hardening behavior, has been observed in numerous experimental studies [24-28]. Wang and Wu [29] and Shan et al. [30] performed axial compression tests on FRP fully confined square concrete columns (FFSC) with varying corner radius ratios $R_r = r/b \geq 0.05$, where b and r denote the cross-section size and corner radius, respectively. Results indicate that reducing R_r from 1 (circular) to 0 (sharp corners) significantly diminishes FRP confinement effectiveness due to horizontal arching and stress concentration at the corners. Low R_r FFSC columns, especially lightly confined HSC/UHSC specimens, are more prone to post-peak strain-softening behavior [18, 31-35]. Similarly, Ozbakkaloglu [13] and Isleem Haytham et al. [1] studied FRP-confined rectangular columns (FFRC) with different aspect ratios R_{sar} = h / b, finding that confinement is less effective than in FFSC because of intensified horizontal arching. As R_{sar} increases, higher FRP stiffness is required to avoid strain-softening [15, 36-38]. In this study, the reduced effectiveness of FRP confinement in non-circular columns (FFSC/FFRC) compared to circular ones (FFCC) is defined as the "Non-circularity Effect," indicating that greater FRP stiffness is needed to achieve a post-peak strain-hardening response.

Numerous models have been developed to predict the axial stress–strain behavior of FRP-confined concrete [39-48], generally classified into analysis-oriented models (AOMs) and design-oriented models (DOMs). AOMs typically involve two steps: (i) determining the FRP confining stress–strain relationship using a dilation model, and (ii) deriving the concrete axial stress from the FRP confining stress via a base model originally developed for actively confined concrete. DOMs, on the other hand, provide a simpler approach through closed-form expressions for critical stress–strain points, calibrated from experimental results. For example, Lam and Teng [49] proposed a parabolic-linear DOM for fully FRP-confined circular concrete (FFCC) specimens with normal-strength concrete (NSC), which Teng et al. [50] later refined using AOM-generated data to update ultimate condition parameters and define a confinement stiffness threshold separating strain-hardening from strain-softening responses. Fallah Pour et al. [51] extended DOM formulations to FFCC specimens with both NSC and high-strength concrete (HSC), though applicability remained limited to strain-hardening behavior. To predict the peak axial compressive strength (f_{cc}) of fully FRP-confined concrete columns, many models have been proposed; however, most are restricted to specific cross-section shapes (circular or square) and often do not account for the full range of geometric and material variations. For fully confined columns, more reliable predictive models can be developed using regression analysis that unifies cross-sectional effects. Some generalized models for fully confined circular (FFCC) and non-circular (FFSC/FFRC) columns have been proposed in the literature (e.g., fib [52], ACI [53]), incorporating confinement efficiency factors to account for vertical and horizontal arching actions. Nevertheless, most existing models were calibrated using limited experimental databases, often covering a narrow range of parameters such as confinement stiffness, concrete strength, and specimen geometry [54]. This restricts their predictive reliability when applied to broader datasets encompassing a wider spectrum of concrete strengths, FRP properties, and column geometries. The accuracy and robustness of regression-based predictive formulations fundamentally depend on the quality, diversity, and comprehensiveness of the experimental database used for calibration. A high-quality database must include a broad range of key parameters (concrete compressive strength, FRP mechanical properties, column geometry, and confinement configurations) to capture both individual and interactive effects on structural behavior. Sparse or biased datasets can lead to models valid only within limited parameter ranges, reducing generalizability and reliability. By contrast, a comprehensive and statistically representative database enables rigorous regression analysis, allowing the derivation of model coefficients that reflect both mean behavior and variability in experimental outcomes. This ensures that the resulting predictive formulation can reliably estimate ultimate axial strength, strain capacity, and full stress–strain behavior for various fully confined concrete columns, while also providing a solid foundation for uncertainty quantification in practical design applications.

In this study, a new design-oriented constitutive model is developed to predict the ultimate compressive strength of circular and non-circular concrete columns confined with FRP jackets. The model is grounded in a physically consistent framework that explicitly accounts for the "Non-circularity Effect", as the progressive loss of confinement efficiency due to cross-sectional geometry, through continuous correction functions of corner radius (R_r) and aspect ratio (R_{sar}). Unlike conventional approaches that treat circular and non-circular sections separately or apply discrete reduction factors, the proposed formulation ensures a smooth transition in predicted strength from circular to square and rectangular geometries, reflecting the underlying mechanics of lateral strain incompatibility and arching action. To support robust regression calibration, an extensive and diverse experimental database of 1723 FRP-confined column tests was compiled, encompassing a wide spectrum of concrete strengths (6.6–204 MPa), FRP material properties (modulus: 13.6–657 GPa; ultimate strain: 0.004–0.037), and geometric configurations (including sharp and rounded corners, and aspect ratios up to 2.0). This database enables the identification of key governing parameters and the development of a unified strength prediction equation that satisfies fundamental physical limits, such as reducing to unconfined strength when confinement stiffness vanishes, and degrading realistically as section shape deviates from circularity. The resulting model is not only statistically validated across all column types but also rigorously tested for parameter sensitivity and boundary consistency, establishing a reliable foundation for both practical design applications and future analytical advancements in FRP-confinement modeling.

2. Research significance

The novelty of the present study lies in its development of a unified, regression-based model for predicting the ultimate compressive strength of FRP-confined concrete columns that explicitly accounts for cross-sectional geometry. Unlike most existing formulations, which either treat circular and non-circular sections separately or rely on ad hoc reduction factors, the proposed model systematically incorporates the mechanics of confinement degradation in non-circular sections through continuous correction functions of corner radius (R_r) and aspect ratio (R_{sar}). This approach ensures a smooth and physically consistent transition in predicted strength from circular to square and rectangular columns, accurately reflecting stress concentrations, lateral strain incompatibility, and horizontal arching effects. The model is calibrated and validated against a large and diverse experimental database of 1,723 FRP-confined column tests, covering a broad range of concrete strengths (6.6–204 MPa), FRP properties (modulus: 13.6–657 GPa; ultimate strain: 0.004–0.037), and geometric configurations, including sharp and rounded corners and aspect ratios up to 2.0. By combining rigorous regression analysis with mechanically grounded correction factors, the study addresses limitations of prior models that were restricted to specific geometries or limited datasets, providing a physically consistent, statistically robust, and practically applicable predictive tool. This advancement bridges the gap between idealized confinement theory and real-world column geometries, offering engineers a unified framework for design and assessment while establishing a foundation for future refinement and recalibration as additional experimental data become available.

3. Compressive behavior of unconfined and FRP-confined concrete

Concrete subjected to axial compressive loading develops a certain level of axial shortening associated with an axial strain εc corresponding to the applied compressive stress f_c. According to Poisson's effect, this axial strain simultaneously generates a lateral (radial) strain $\varepsilon_l = \nu \times \varepsilon_c$, where ν is the Poisson's ratio. The continuous increase of lateral dilation during loading initiates internal microcracking, which subsequently evolves into visible cracking within the concrete matrix [38, 55]. As illustrated in Fig. 1, the stress–strain response ($f_c - \varepsilon_c$) of unconfined concrete is initially linear up to approximately 50% of its peak compressive strength ($0.5f_{c0}$). In this linear region, the slope of the curve corresponds to the elastic modulus of concrete E_c. Beyond this linear-elastic range and up to the peak stress (f_{cc}), diagonal and longitudinal microcracks begin to form and grow, causing the ascending branch of the $f_c - \varepsilon_c$ curve to deviate from linearity. This deviation is characterized by a gradual reduction in tangent stiffness due to progressive internal damage and stiffness degradation. The axial strain corresponding to the peak compressive stress, denoted as ε_{c0}, is commonly assumed to be approximately 0.002 for normal-strength unconfined concrete [56, 57]. After reaching this peak, concrete exhibits no further capacity to resist additional compressive load, and the widening of diagonal and longitudinal cracks becomes more pronounced. Consequently, the compressive stiffness drops significantly, and the stress–strain curve transitions into a descending (softening) branch, marking the onset of brittleness and instability within the concrete. This post-peak softening behavior is a fundamental characteristic of unconfined concrete and is closely associated with unstable crack propagation, volumetric expansion, and rapid loss of load-carrying capacity.

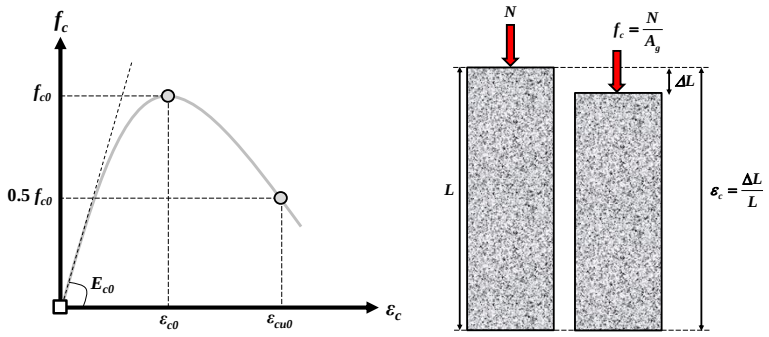

Fig. 1. Axial behavior of unconfined concrete.

The confinement mechanism developed in FRP-jacketed concrete columns is fundamentally governed by the interaction between the axial compression-induced dilation of concrete and the tensile resistance of the surrounding FRP jacket [58]. When the concrete is subjected to an axial compressive strain ε_c, a corresponding lateral (radial) strain $\varepsilon_l = \nu \times \varepsilon_c$ is generated due to Poisson's effect, where ν denotes the Poisson's ratio of uncracked concrete (Fig. 2). This lateral strain, which arises from the volumetric expansion of the concrete core, directly transforms into hoop strain in the confining jacket because, under perfect confinement conditions, the radial strain of the concrete is equal to the hoop strain of the jacket ($\varepsilon_h = \varepsilon_l$) [49]. Assuming full strain compatibility at the concrete–FRP interface (an assumption widely adopted in confinement mechanics due to the high stiffness and minimal slip of bonded FRP systems), the induced hoop strain in the concrete is transmitted to the FRP jacket as tensile hoop strain $\varepsilon_{h,f}$. Therefore, $\varepsilon_{h,f} = \varepsilon_h = \varepsilon_l = \nu \times \varepsilon_c$. Consequently, generating a certain axial strain in the concrete necessarily requires the development of a proportional tensile strain in the FRP jacket, which in turn mobilizes a tensile stress $f_f = E_f \times \varepsilon_{h,f}$. The tensile stress carried by the FRP is then converted into an effective lateral confining pressure $f_{l,f}$ acting on the concrete core. This pressure acts in opposition to the dilation of the concrete and effectively suppresses the transversal expansion that drives microcracking and loss of stiffness. From a mechanical standpoint, this process implies that, under axial compression, an FRP-confined concrete element must attain a higher axial compressive stress f_c than an unconfined concrete element to reach the same levels of axial and lateral strain. The additional axial stress reflects the work required to engage the FRP jacket in tension and develop the confinement pressure. As loading progresses, the confinement pressure increases approximately in proportion to the tensile strain in the FRP, leading to a triaxial state of stress

within the concrete. This triaxial confinement delays crack propagation, enhances compressive strength, and significantly improves post-peak ductility. The overall effect of the FRP jacket, therefore, is to constrain both axial shortening and lateral dilation of the concrete, mitigating the mechanisms that otherwise lead to rapid stiffness degradation and brittle collapse. This interaction, where axial compression induces lateral tension in the confining system, which in turn provides radial restraint, is the essence of the FRP confinement mechanism.

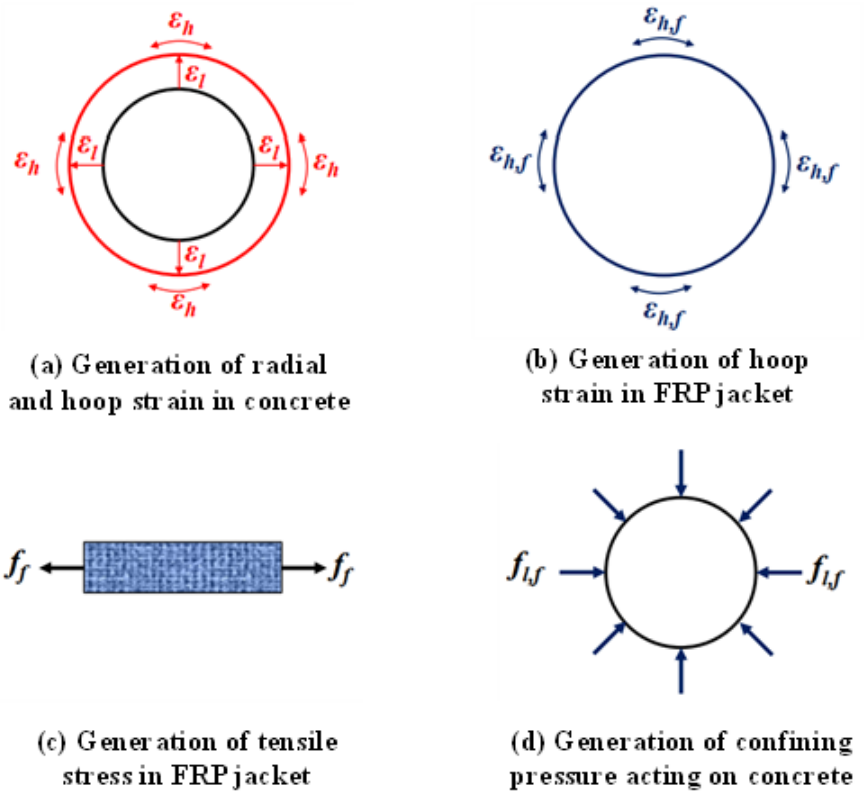

Fig. 2. FRP confinement mechanism.

4. General structure of regression-based formulation

In regression-based models, the normalized compressive strength of FRP-confined concrete is typically expressed as a function of key confinement and material parameters. In general, the normalized compressive strength of FRP-confined concrete can be expressed in a generic form as:

$$\frac{f_{cc}}{f_{c0}} = 1 + \Delta_f \tag{1}$$

Where Δ_f represents the confinement-induced strength gain beyond the unconfined capacity f_{c0}. To obtain a formulation suitable for regression analysis (and to explicitly express Δ_f as a function of the governing parameters), the above relation is rearranged into the standard predictive format:

$$\frac{f_{cc}}{f_{c0}} = \Delta_f \geq 1 \tag{2}$$

Experimental evidence indicates that the compressive strength of axially loaded FRP-confined circular concrete columns is governed primarily by four key parameters [32, 34, 59]: (1) the confinement stiffness of the FRP system, (2) the ultimate tensile strain of the FRP jacket, (3) the compressive strength of the unconfined concrete, and (4) the column dimension size. Considering the key mechanical factors affecting the confinement mechanism, the following general form is proposed for the regression-based predictive model:

$$\frac{f_{cc}}{f_{c0}} = \beta_1 {K_L}^{\beta_2} {\varepsilon_{fu}}^{\beta_3} {f_{c0}}^{\beta_4} {R_b}^{\beta_4} \geq 1 \tag{3}$$

in which

$$K_L = 2\frac{n_f t_f E_f}{b} \tag{4}$$

where β_1 to β_4 are empirical regression coefficients whose values will be calibrated using the constructed experimental database in the next sections. ($R_b = b/150$) denotes the normalized column dimension size, introduced to capture size-dependent confinement

efficiency. K_L is the FRP confinement stiffness, a parameter widely recognized as the dominant factor governing strength enhancement in FRP-confined concrete. εfu is the ultimate hoop tensile strain of the FRP jacket.

It should be emphasized that the influence of column non-circularity is incorporated into the proposed formulation through physically motivated reduction factors applied to the confinement efficiency coefficient β_1. These reduction factors are expressed as continuous functions of the sectional aspect ratio and the corner radius ratio, which are the primary geometric parameters governing stress concentration at corners, non-uniform lateral confining pressure, and the presence of ineffective confinement zones in non-circular sections. By modifying β_1, the formulation directly reduces the effective confinement contribution provided by the FRP jacket, thereby reflecting the progressive loss of confinement efficiency as the cross-section deviates from a circular shape.

In addition, the proposed model satisfies essential physical boundary conditions. In the absence of effective confinement, represented by a vanishing confinement stiffness ($K_L \rightarrow 0$), the contribution of the FRP jacket diminishes, and the formulation correctly reduces to unity, indicating no confinement-induced strength enhancement. This behavior ensures consistency with unconfined concrete mechanics and confirms that the proposed expression is grounded in physical principles rather than purely empirical fitting.

5. Test database of FRP-confined concrete columns

In this study, an extensive experimental database was compiled from previously published test results reported in the literature as shown in Table 1. The database consists of concrete column specimens tested under concentric axial compressive loading and confined with externally bonded FRP jackets. No new experimental testing was conducted as part of the present work. To ensure a consistent, reliable, and unified database suitable for regression-based modeling, strict selection criteria were applied. Specimens containing conventional steel longitudinal or transverse reinforcement were excluded, as were specimens with partial confinement configurations or spiral wrapping systems. Tests in which FRP debonding governed the failure mode were not considered, nor were specimens confined using hybrid FRP systems composed of different fiber types. Columns subjected to eccentric axial loading were excluded to eliminate secondary bending effects. Experimental results for which the ultimate compressive strength of the confined specimen was lower than that of the corresponding unconfined concrete ($f_{cc} < f_{c0}$) were also excluded. Only specimens confined with FRP materials exhibiting linear tensile stress–strain behavior (namely CFRP, GFRP, BFRP, and AFRP) were included in the database. Specimens confined with PEN- or PET-based fibers, which exhibit nonlinear tensile behavior, were excluded to maintain material consistency across the dataset. The application of these criteria resulted in a comprehensive and internally consistent database of 1,723 test specimens, providing a reliable basis for model development and validation.

Analysis of the unconfined concrete strength (f_{c0}) indicates a wide range from 6.6 MPa to 204 MPa, with mean values of 45–48 MPa for circular and combined cross-section datasets, and slightly lower mean values for square (33.5 MPa) and rectangular (37.5 MPa) columns. The confined concrete strength (f_{cc}) ranges from 14.5 MPa to 381 MPa, yielding normalized strength ratios (f_{cc} / f_{c0}) from 1.02 to 6.9. Circular columns generally show a higher mean normalized strength (≈ 2.03) compared to square (1.63) and rectangular (1.27) columns, confirming the stronger confinement efficiency of circular geometries. Column dimensions in the dataset cover a substantial range: heights (L) from 100 mm to 1,200 mm and cross-sectional dimensions (b) from 50 mm to 400 mm. The FRP properties are equally diverse, with modulus of elasticity (E_f) varying from 13.6 GPa to 657 GPa and effective thickness ($n_f \times t_f$) from 0.004 mm to 9.754 mm. The ultimate FRP strain (ε_{fu}) spans 0.004–0.037, reflecting the range of fiber types and material qualities considered in the experiments. The coefficient of variation (CoV) for most parameters is significant, indicating considerable scatter in material properties, column dimensions, and FRP characteristics. This variability emphasizes the need for regression-based models that can capture the effects of both material and geometric parameters. Shape- and size-related factors (R_r and R_{sar}) show that correction factors can vary from 0.00 to 2.0, highlighting the impact of geometry and aspect ratio on confinement efficiency. The analysis of the compiled database demonstrates that FRP confinement substantially enhances the compressive strength of concrete, with circular columns showing the highest confinement efficiency, followed by square and rectangular sections. The dataset covers a wide range of concrete strengths, column sizes, FRP properties, and ultimate strains, providing significant variability that reflects realistic experimental conditions. This diversity ensures that the database is comprehensive and suitable for developing robust regression-based predictive models. The observed trends, including the influence of cross-sectional shape, FRP thickness, and material stiffness, highlight the critical parameters that govern the behavior of FRP-confined concrete. Overall, the database offers a solid foundation for accurate strength prediction, model validation, and future parametric studies of FRP confinement effects.

Table 1. Details of the test database of FRP-confined circular/non-circular concrete columns.

Cross-Section type	No. of Data	Statistical Index	f_{c0} (MPa)	f_{cc} (MPa)	f_{cc} / f_{c0}	L (mm)	b (mm)	E_f (GPa)	$n_f \times t_f$ (mm)	ε_{fu}	R_r	R_{sar}
Circle, Square & Rectangle	1723	Minimum	6.6	14.5	1.02	100	50	13.6	0.057	0.004	0.07	1
		Maximum	204	381	6.9	1200	400	657	9.75	0.037	1	2
		Mean	45.8	79.7	1.92	327	147.5	193.7	0.58	0.018	0.87	1.05
		Cov	0.7	0.42	0.61	0.42	0.31	0.48	1.29	0.3	0.3	0.19
Circle	1376	Minimum	6.6	17.8	1.05	100	50	13.6	0.057	0.004	1	1
		Maximum	204	381	6.9	915	305	657	5.1	0.037	1	1
		Mean	48.5	87.4	2.03	301	144	190	0.581	0.018	0	0

		Cov	0.71	0.58	0.41	0.37	0.31	0.52	1.19	0.32	0	0
Square	216	Minimum	8.7	14.5	1.05	200	100	13.6	0.117	0.009	0.07	1
		Maximum	77.2	114	4.32	1200	400	260	9.754	0.031	0.8	1
		Mean	33.5	51.2	1.63	419	172	204	0.596	0.004	0.35	0
		Cov	0.41	0.34	0.33	0.4	0.32	0.33	1.56	0.2	0.52	0
Rectangle	131	Minimum	17.3	20.3	1.02	300	90	16.3	0.13	0.014	0.14	1.25
		Maximum	79.6	95.9	2.54	1000	203	257	9.754	0.021	0.67	2
		Mean	37.5	46	1.27	442	141	219	0.573	0.017	0.38	1.71
		Cov	0.43	0.36	0.2	0.43	0.21	0.25	1.64	0.1	0.36	0.16

6. Proposed formula for non-circular FRP-confined concrete columns

In the present study, the experimental data from the database were used to determine the coefficients of Eq. 3. Based on 1,376 experimental specimens of 'circular' concrete columns, a relationship between the ratio of the maximum compressive strength of confined concrete (f_{cc} / f_{c0}) and the key parameters ε_{fu}, K_L, f_{c0} and R_b is proposed as follows:

$$\frac{f_{cc}}{f_{c0}} = 3.1{K_L}^{0.36}{\varepsilon_{fu}}^{0.23}{f_{c0}}^{-0.55}{R_b}^{-0.14} \geq 1 \tag{5}$$

Based on the experimental results reported by Wang and Wu [29], the effect of confinement in enhancing the axial behavior of concrete columns with square cross-sections is less pronounced than in columns with circular cross-sections. This is due to the stress concentration at the corners of the square section, which reduces the effectiveness of confinement in controlling the lateral expansion of concrete. Moreover, because of the horizontal arching action in the confinement mechanism, some regions of the cross-section experience ineffective confinement. Consequently, the axial behavior of the concrete in these regions is similar to that of unconfined concrete. An experimental study conducted by Shan et al. [30] showed that with increasing corner radius r of non-circular sections, from $r = 0$ (representing a square section with sharp corners) to $r = 2b$ (representing a circular section), the effectiveness of FRP confinement improves. In the present study, to investigate the effects of this parameter, Eq. 5, which was originally proposed exclusively for circular sections, was used to predict the maximum confined compressive strength (f_{cc} / f_{c0}) of square concrete columns. Fig. 3a illustrates the relationship between the analytical-to-experimental results ($\beta_r = f_{cc} / f_{c0}$) and the corner radius factor ($R_r = 2r / b$) based on 216 experimental specimens. As can be observed, reducing R_r from 1 (representing a circular section) to values close to zero leads to non-conservative predictions for square columns. The dependence of the error (β_r) on R_r indicates that the experimental results are a function of the corner radius, and therefore, the effects of section rounding must be considered in the analytical model. By performing regression analysis on the 216 experimental data points of FRP-confined square columns, the relationship between the error (β_r) and R_r was obtained as follows:

$$\beta_r = \frac{{f_{cc}}^{Ana}}{{f_{cc}}^{Exp}} = 0.91{R_r}^{-0.34} \geq 1 \tag{6}$$

Therefore, by substituting Eq. 6 into Eq. 5, the proposed formula for square concrete columns confined with FRP jackets is obtained as follows:

$$\frac{f_{cc}}{f_{c0}} = \frac{3.1}{\beta_r}{K_L}^{0.36}{\varepsilon_{fu}}^{0.23}{f_{c0}}^{-0.55}{R_b}^{-0.14} \geq 1 \tag{7}$$

Based on the statistical indices, as shown in Fig. 3b, Eq. 7 provides accurate predictions of the maximum compressive strength of square concrete columns confined with FRP jackets. Fig. 3c illustrates the relationship between the prediction error of Eq. 7 and the corner radius factor. As can be observed, after applying the correction factor in the proposed equation, the resulting error shows no correlation with the factor (R_r), indicating that the effects of this parameter have been correctly captured in the proposed formula.

Based on the experimental results reported by Ozbakkaloglu [13], and Triantafillou et al. 2016, the effect of FRP confinement on concrete columns with rectangular cross-sections is smaller compared to circular and square columns. Even for rectangular columns with an aspect ratio ($R_{sar} = h / b$) greater than approximately 2, the effects of confinement on concrete behavior are almost negligible. The primary reason is the significant negative influence of the horizontal arching action within the confinement mechanism. Consequently, most regions of the cross-section are subjected to ineffective confinement and exhibit behavior similar to unconfined concrete under axial loading. As a result, increasing R_{sar} from a value of 1 (with $R_{sar} = 1$ representing a square column) reduces the effectiveness of FRP confinement on rectangular concrete columns.

In this study, to investigate the effects of the R_{sar} parameter, Eq. 7, which was originally proposed exclusively for circular/square sections, was used to predict the maximum confined compressive strength (f_{cc} / f_{c0}) of rectangular concrete columns. Fig. 4a shows the relationship between the analytical-to-experimental results ($\beta_{sar} = {f_{cc}}^{Ana} / {f_{cc}}^{Exp}$) and the aspect ratio R_{sar} based on 131 experimental specimens. As can be seen, increasing R_{sar} from 1 (representing a square section) leads to non-conservative predictions for rectangular columns. The dependence of the error (β_{sar}) on R_{sar} indicates that the experimental results are a function of the aspect ratio, and therefore, the effects of R_{sar} must be considered in the analytical model.

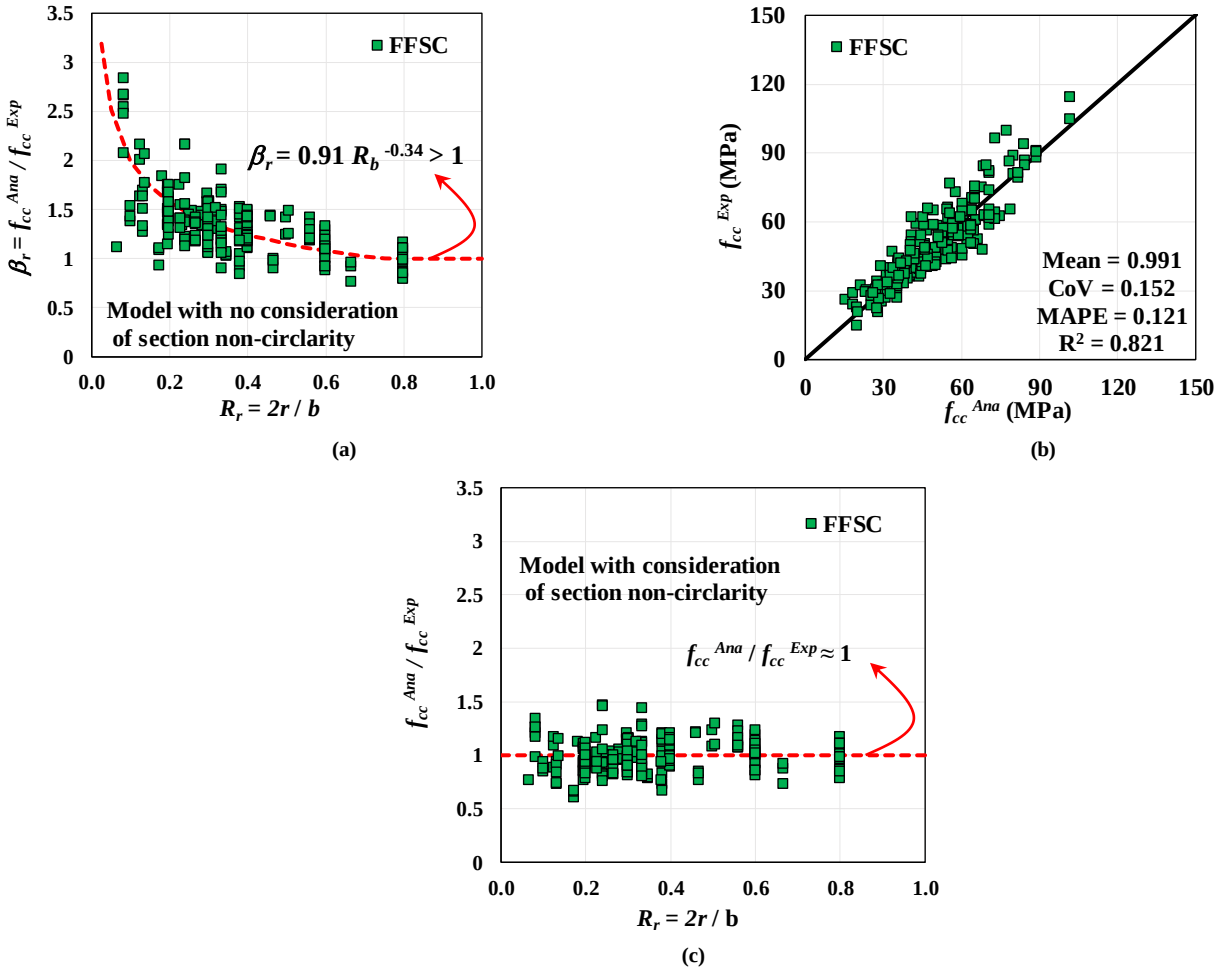

Fig. 3. Evaluation of the predicted results from the proposed model for f_{cc} of square columns based on 216 test specimens.

By performing regression analysis on the 131 experimental data points of FRP-confined rectangular columns, the relationship between the error (β_{sar}) and R_{sar} was obtained as follows:

$$\beta_{sar} = \frac{f_{cc}^{Ana}}{f_{cc}^{Exp}} = 0.95 {R_{sar}}^{0.78} \geq 1 \tag{8}$$

Therefore, by substituting Eq. 8 into Eq. 7, the proposed formula for rectangular concrete columns confined with FRP jackets is obtained as follows:

$$\frac{f_{cc}}{f_{c0}} = \frac{3.1}{\beta_r \beta_{sar}} {K_L}^{0.36} {\varepsilon_{fu}}^{0.23} {f_{c0}}^{-0.55} {R_b}^{-0.14} \geq 1 \tag{9}$$

Based on the statistical indices, as shown in Fig. 4b, Eq. 9 provides accurate predictions of the maximum compressive strength of rectangular concrete columns confined with FRP jackets. Fig. 4c illustrates the relationship between the prediction error of Eq. 9 and the aspect ratio factor R_{sar}. As can be observed, after applying the β_{sar} correction factor in the proposed equation, the resulting error shows no significant correlation with β_{sar}, indicating that the effects of this parameter have been correctly captured in the proposed formula.

It should be emphasized that Eq. 9 is formulated to be universally applicable to all column shapes, including circular, square, and rectangular sections. This generality is particularly important because the confinement effectiveness of FRP jackets is strongly influenced by cross-sectional geometry, corner rounding, and aspect ratio, which can vary significantly across different column shapes. To assess the robustness and predictive capability of the proposed formula, its performance was evaluated using the entire experimental database, encompassing 1,723 specimens with a wide range of dimensions, material properties, and FRP configurations.

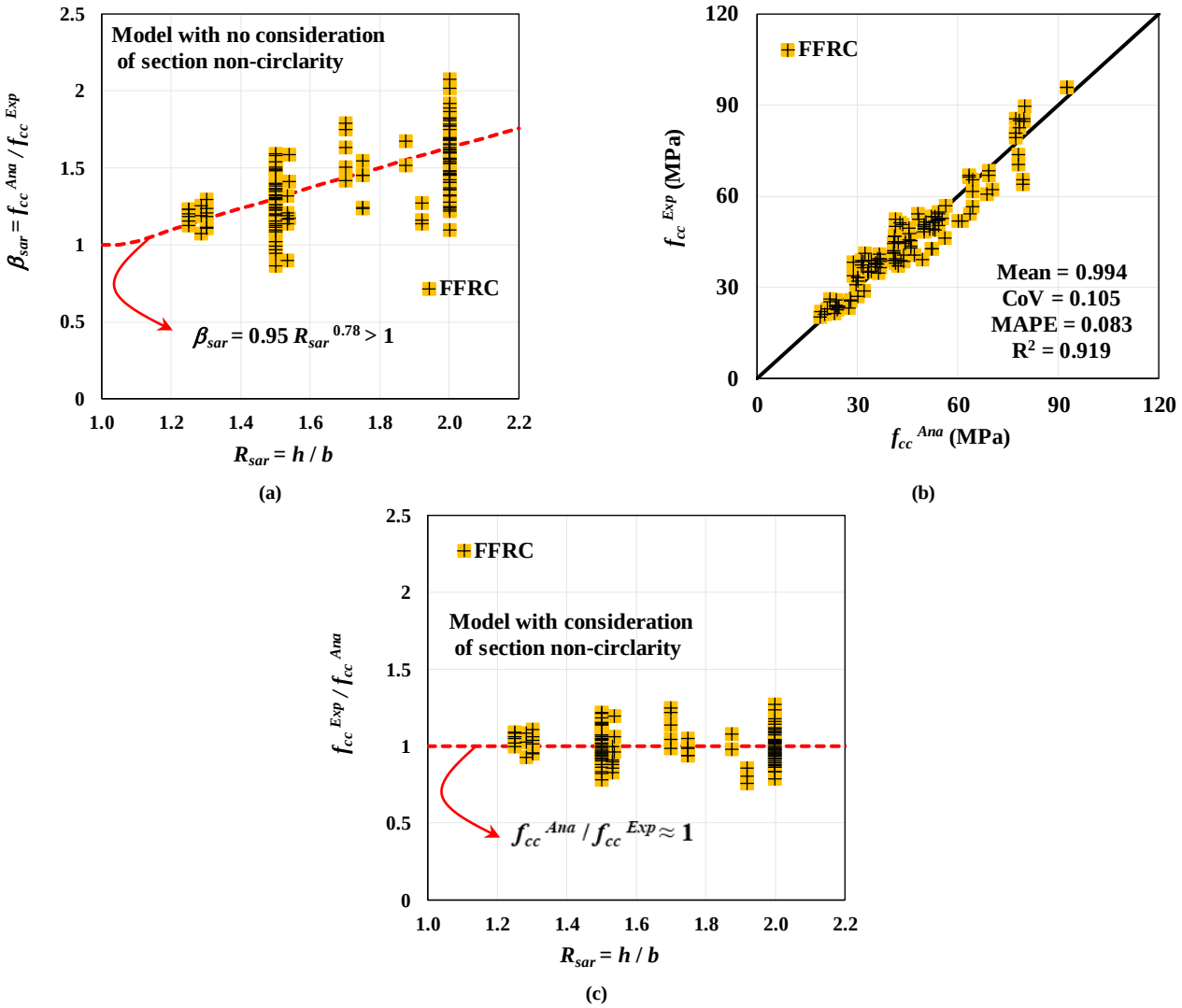

Fig. 4. Evaluation of the predicted results from the proposed model for the maximum compressive strength of rectangular columns based on 131 experimental specimens.

Fig. 5 presents a comparison between the experimental results and the predictions obtained using Eq. 9. The figure demonstrates a strong correlation between the predicted and measured maximum compressive strengths across all column shapes. Statistical indicators, including mean error, standard deviation, and coefficient of variation, confirm that the proposed formula provides accurate and reliable predictions for a diverse set of experimental conditions. In particular, the formula successfully captures the variations in confinement effectiveness due to cross-sectional shape and aspect ratio, which have been identified as critical factors in previous studies. The high accuracy of Eq. 9 is significant for several reasons. First, it allows structural engineers and researchers to reliably estimate the ultimate strength of FRP-confined concrete columns without the need for extensive experimental testing, reducing both cost and time. Second, its applicability across multiple geometries ensures that the formula can be used in practical design scenarios, where columns may not always be perfectly circular or square. Finally, the validation against a large experimental database demonstrates the robustness of the model, highlighting its potential for use in design codes and guidelines for FRP-confined concrete structures. Overall, Eq. 9 provides a comprehensive and versatile predictive tool for evaluating the axial performance of FRP-confined concrete columns under a wide range of conditions.

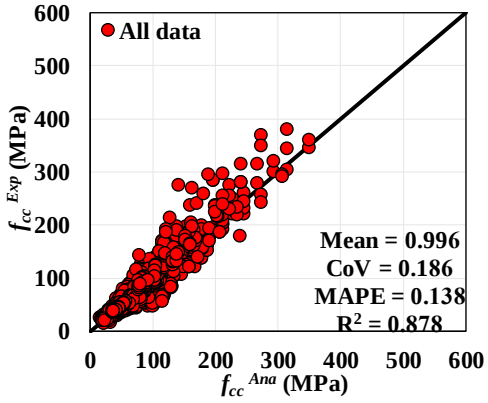

Fig. 5. Comparison of the predicted maximum compressive strength of circular, square, and rectangular columns using the proposed model based on 1,723 experimental specimens.

7. Comparison of the proposed model with existing models

7.1. Circular concrete columns

Table 2 compares the predictions of circular FRP-confined concrete columns from existing analytical models [39, 40, 52, 53, 60] and the proposed model. Statistical indices include MAPE, MSE, CoV, MV, and R^2. Among the existing models, the fib [52] model demonstrates the best performance, with relatively low error and variability (MV = 0.892, CoV = 0.226), although it slightly underestimates the experimental data. In contrast, Cao et al. [39] produces non-conservative predictions with high scatter. The proposed model consistently outperforms all existing models across these indices. This superior performance is attributable to several factors. First, the large and diverse experimental database used for calibration, covering a wide range of concrete strengths, FRP properties, and column dimensions, provides a robust foundation for accurately capturing confinement behavior. Unlike many existing models, which were calibrated for a limited concrete class or narrower dataset, the proposed model explicitly incorporates the effect of the unconfined concrete strength on the confinement response. Second, the model incorporates physically consistent relationships between the FRP confinement and concrete response, including FRP stiffness, ultimate strain, and column diameter. The combined consideration of unconfined concrete strength and FRP properties ensures accurate prediction across the full spectrum of material strengths. In contrast, existing models are often less generalizable, performing reliably only for the concrete classes and column sizes represented in their original calibration datasets.

7.2. Square concrete columns

Table 3 presents the comparison for square columns. Both the proposed model and Cao et al. [39] perform well, but the proposed model provides consistently accurate predictions across all 216 specimens. Other models, such as Guo et al. [40], produce overly conservative predictions with high scatter. Mechanistically, the superior performance of the proposed model is rooted in both its large, diverse experimental database and its physically consistent treatment of geometric effects. The database of 1,723 specimens spans circular, square, and rectangular columns with a wide range of aspect ratios and corner radius ratios, providing sufficient coverage to calibrate the influence of non-circularity accurately. The proposed model incorporates continuous geometric correction factors based explicitly on sectional aspect ratio and corner radius, allowing it to reflect the progressive reduction in confinement efficiency caused by corner stress concentrations, non-uniform lateral pressure distribution, and partially ineffective confinement zones. In contrast, most existing models were developed using smaller, less diverse datasets, often dominated by circular sections, and typically incorporate geometric effects through simplified or discrete reduction factors. This limits their ability to capture the nuanced impact of cross-sectional shape on confinement performance, leading to either overly conservative or non-conservative predictions for non-circular columns. By combining a large, representative database with continuous, mechanistically motivated geometric corrections, the proposed model achieves consistently accurate and robust predictions across all column geometries.

7.3. Rectangular concrete columns

Table 4 summarizes the comparison for rectangular columns. Again, the proposed model and Cao et al. [39] show the best performance, with the proposed model providing slightly more precise predictions for the 131 experimental specimens. The proposed model maintains low MAPE and MSE values while achieving high R^2, demonstrating its ability to capture the effects of aspect ratio and cross-sectional geometry accurately. Other models, particularly Guo et al. [40], perform poorly with highly conservative predictions and large scatter. This improved performance of the proposed model stems from its explicit consideration of section aspect ratio and corner radius, which govern the distribution of lateral confinement, stress concentrations at corners, and partially ineffective confinement zones. Existing models often use simplified or discrete reduction factors and were calibrated with smaller datasets, limiting their ability to represent continuous variations in confinement efficiency for high aspect ratios. By contrast, the proposed model applies continuous geometric correction factors, enabling it to accurately capture the gradual decrease in confinement effectiveness as the rectangular section becomes more elongated, while also accounting for the influence of the unconfined concrete strength and FRP properties on axial compressive behavior.

7.4. Overall performance across all column shapes

Table 5 compares the predictions of all models against the full experimental dataset of 1,723 specimens encompassing circular, square, and rectangular columns. The fib [52] model performs well but slightly underestimates the experimental data, while Guo et al. [40] is the least accurate, producing highly conservative predictions. The proposed model consistently achieves high accuracy across all column shapes, with low MAPE, MSE, and CoV values and R^2 close to 0.92, demonstrating its robustness and reliability. This uniform performance is attributable to the model's mechanistic incorporation of geometric effects through continuous aspect ratio and corner radius correction factors, along with explicit consideration of unconfined concrete strength, FRP stiffness, and ultimate FRP strain. Unlike many existing models, which may be accurate only within the limited geometries and material ranges used for their calibration, the proposed model captures the combined influence of section shape, size, and material properties. This demonstrates that its improved predictive performance is not solely due to the larger database but is fundamentally based on a physically grounded and unified formulation, enabling robust and reliable predictions for arbitrary column geometries.

Table 2. Comparison of existing analytical models predictions of ultimate strength for circular FRP-confined concrete columns.

Analytical Model	R^2	MAPE	MSE	CoV	MV
ACI [53]	0.812	0.189	0.375	0.279	0.938
fib [52]	0.82	0.185	0.343	0.226	0.892
Cao et al. [39]	0.782	0.257	1.03	0.313	1.219

Wei and Wu [60]	0.812	0.189	0.426	0.282	1.078
Guo et al. [40]	0.82	0.266	0.628	0.252	0.77
Proposed Model	0.865	0.145	0.202	0.197	0.996

Table 3. Comparison of existing analytical models predictions of ultimate strength for square FRP-confined concrete columns.

Analytical Model	R^2	MAPE	MSE	CoV	MV
ACI [53]	0.909	0.212	0.167	0.164	0.679
fib [52]	0.895	0.18	0.18	0.153	0.782
Cao et al. [39]	1.05	0.156	0.085	0.132	0.824
Wei and Wu [60]	0.994	0.163	0.102	0.124	0.796
Guo et al. [40]	0.788	0.2	0.336	0.229	0.671
Proposed Model	0.991	0.152	0.076	0.121	0.821

Table 4. Comparison of existing analytical models predictions of ultimate strength for rectangular FRP-confined concrete columns.

Analytical Model	R^2	MAPE	MSE	CoV	MV
ACI [53]	1.046	0.141	0.037	0.128	0.857
fib [52]	1.02	0.154	0.037	0.133	0.873
Cao et al. [39]	1.044	0.113	0.026	0.105	0.93
Wei and Wu [60]	1.122	0.116	0.044	0.144	0.919
Guo et al. [40]	1.338	0.258	0.367	0.351	0.688
Proposed Model	0.994	0.105	0.018	0.083	0.919

Table 5. Comparison of existing analytical models predictions of ultimate strength for circular/square/rectangular FRP-confined concrete columns.

Analytical Model	R2	MAPE	MSE	CoV	MV
ACI [53]	0.943	0.264	0.323	0.181	0.825
fib [52]	0.902	0.218	0.299	0.177	0.833
Cao et al. [39]	1.184	0.299	0.832	0.229	0.805
Wei and Wu [60]	1.071	0.263	0.355	0.177	0.83
Guo et al. [40]	0.816	0.314	0.571	0.268	0.795
Proposed Model	0.996	0.186	0.173	0.138	0.878

8. Error analysis of the proposed model based on key parameters

To further assess the accuracy of the proposed model in predicting the maximum compressive strength of FRP-confined concrete columns, the ratio of analytical results to experimental data ($Y = f_{cc}^{Ana}/f_{cc}^{Exp}$) was analyzed for 1,723 experimental specimens. The variation of Y with respect to key parameters (X) is illustrated in Fig. 6. Here, Fig. 6a shows the relationship between Y and the lateral confinement stiffness parameter (K_L). Regression analysis yields $Y = 0.9811+1\times10^{-5}\,X$. The near-zero coefficient and very low R^2 indicate that the prediction error of the proposed model is independent of the stiffness level of the FRP confinement. This demonstrates that the model accurately captures the influence of confinement stiffness on the maximum compressive strength of FRP-confined columns. Fig. 6b presents Y versus the unconfined concrete compressive strength (f_{c0}). Regression produces $Y = 0.9948+2\times10^{-5}\,X$. Again, the coefficient is near zero and R^2 is minimal, indicating that the model error is independent of concrete strength. This confirms that the proposed model can accurately simulate the effect of different concrete strength levels, including low-, normal-, high-, and ultra-high-strength concrete, on the confined column strength. Fig. 6c illustrates Y as a function of the FRP ultimate tensile strain (ε_{fu}), giving $Y = 0.9347+3.3629X$. The very low coefficient and R^2 confirm minimal error dependency on FRP strain. However, for small values of $\varepsilon_{fu} \leq 0.005$, corresponding to high-modulus FRP sheets, the model slightly overestimates strength. For such cases, a reduction factor of approximately 0.66 is recommended. Overall, the proposed model correctly captures the influence of FRP strain on column strength. The effect of column dimensions, expressed as $X = b/150$, is shown in Fig. 6d. Regression yields $Y = 1.0271-0.0322X$. The near-zero coefficient and very low R^2 indicate that the model's error is not dependent on column size, confirming that the model properly accounts for geometric effects. Fig. 6e presents the relationship between Y and the corner radius of non-circular sections ($R_r = 2r/b$), giving Y=0.9814+0.0162X. The low coefficient and R^2 show negligible error dependency on corner rounding, demonstrating that the model can accurately simulate the effect of corner radius on the maximum compressive strength. Finally, Fig. 6f shows Y versus the section aspect ratio (h/b), with regression $Y = 0.9948+2\times10^{-5}\,X$. Again,

the near-zero coefficient and very low R^2 indicate that the model error is independent of the aspect ratio, confirming the model's ability to account for cross-sectional geometry effects. Overall, the analysis indicates that among all parameters, the FRP ultimate tensile strain exhibits the highest influence on prediction error ($R^2 = 0.0097$), whereas the unconfined concrete strength shows the least dependency ($R^2 \approx 7\times10^{-5}$). These results demonstrate that the proposed model reliably predicts the maximum compressive strength of FRP-confined concrete columns while accurately simulating the effects of key material and geometric parameters.

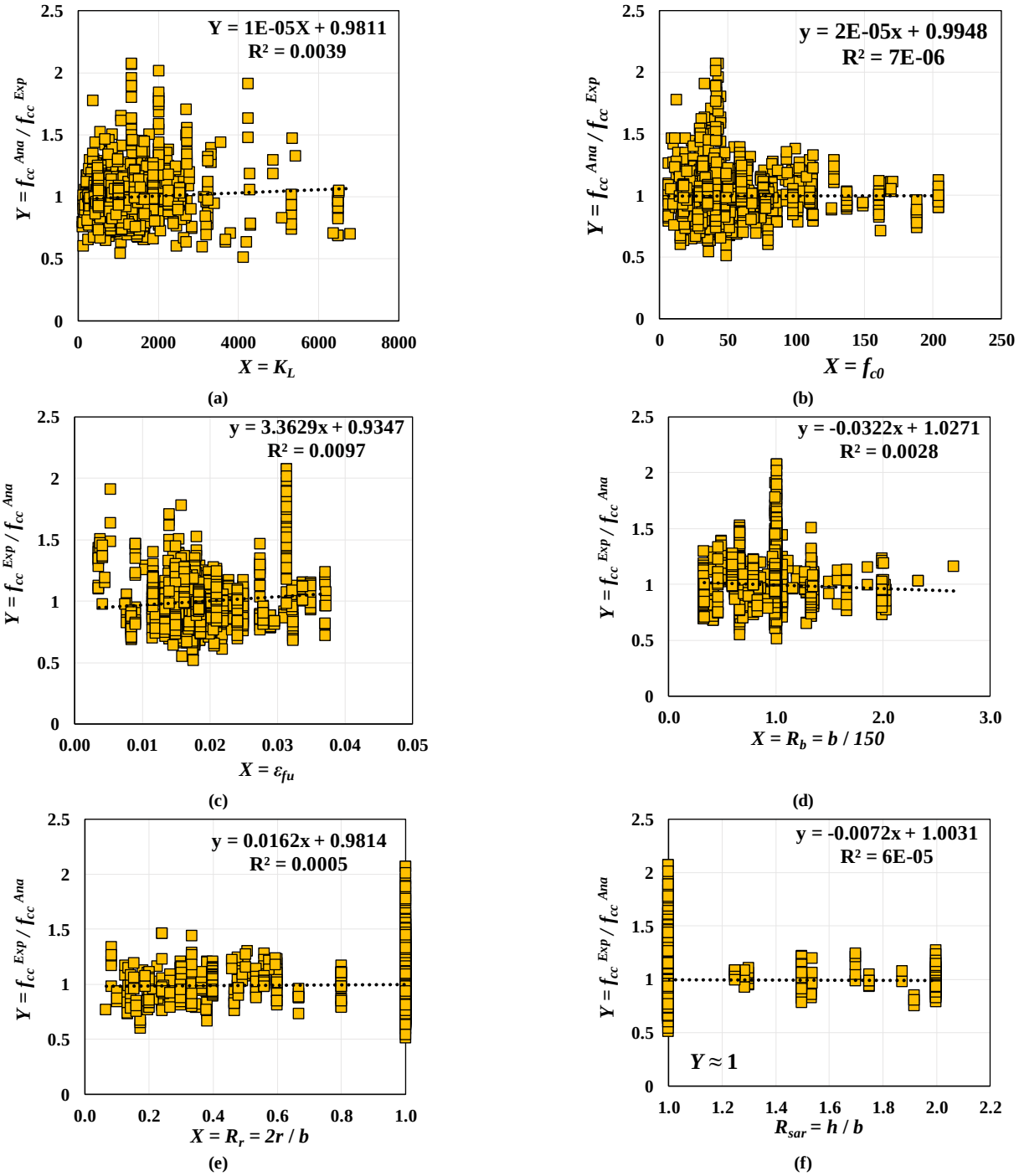

Fig. 6. Ratio of analytical to experimental results for 1,723 specimens, shown against key parameters affecting FRP confinement.

9. Conclusion

This study develops and validates a unified, regression-based model for predicting the compressive strength of FRP-confined concrete columns, explicitly considering the effects of cross-sectional geometry. The key contributions and findings are summarized as follows:

- Unified modeling approach: The proposed model provides a single, coherent framework applicable to circular, square, and rectangular columns, systematically integrating the influence of cross-sectional geometry on FRP confinement effectiveness. This unification ensures consistent predictive capability across diverse shapes, capturing both the enhanced confinement in circular sections and the reduced effectiveness in non-circular, cornered, or elongated geometries without requiring separate, shape-specific equations.

- Mechanically grounded correction factors: The model incorporates continuous, physically motivated correction factors for corner radius (R_r) and section aspect ratio (R_{sar}), which explicitly account for stress concentrations, non-uniform lateral pressure, and reduced arching action in non-circular sections. This approach provides a mechanistically justified representation of geometric effects, avoiding the need for ad hoc or arbitrary shape factors commonly used in previous models.
- Stepwise calibration: The model was developed in a systematic, stepwise manner, starting with a baseline formulation derived from 1,376 circular column specimens and subsequently extended to 216 square and 131 rectangular specimens. This approach ensures that critical physical mechanisms (such as stress concentrations at sharp corners and reduced arching action in elongated sections) are explicitly captured in the predictive equations, rather than being averaged out or obscured by purely empirical fitting.
- Extensive validation: The model was rigorously validated against a comprehensive experimental database of 1,723 specimens, spanning concrete strengths from 6.6 to 204 MPa, FRP moduli from 13.6 to 657 GPa, ultimate strains from 0.004 to 0.037, and column dimensions from 50 to 400 mm. It demonstrates high predictive performance (R^2 = 0.996, MAPE = 18.6%, CoV = 0.138) and consistently outperforms existing analytical and empirical models across circular, square, and rectangular sections, confirming both its accuracy and generalizability.
- Physical consistency: The model rigorously satisfies fundamental mechanical limits. It correctly reduces to the unconfined concrete strength as the FRP confinement stiffness $KL \rightarrow 0$, ensuring no artificial strength enhancement is predicted in the absence of confinement. For non-circular sections, it captures the progressive and physically realistic degradation of confinement effectiveness, reflecting the combined effects of corner stress concentrations, reduced arching action, and non-uniform lateral pressure. This allows smooth transitions in predicted strength from circular sections (maximal confinement efficiency) to square sections and further to increasingly slender rectangular geometries, maintaining a consistent and mechanically justified representation of how cross-sectional shape influences FRP confinement performance.
- Applicability and limitations: As with any regression-based model, predictive accuracy is limited by the quality and range of the database used; if a more extensive or diverse experimental dataset becomes available, the model can be recalibrated to extend its applicability. The current model is based on fully wrapped, axially loaded concrete columns confined with FRP materials exhibiting linear tensile behavior (CFRP, GFRP, BFRP, AFRP) and does not cover columns with eccentric loading, partial or spiral confinement, hybrid FRP systems, or FRP materials with nonlinear tensile behavior (e.g., PEN- or PET-based fibers). Specimens in which FRP debonding governed failure were excluded, so predictions for such cases may be less reliable. For very high-modulus, low-ductility FRP systems ($\varepsilon_{fu} \leq 0.005$), a conservative reduction factor (~0.66) is recommended.
- Practical significance: The model offers engineers a unified, closed-form predictive tool that seamlessly bridges idealized confinement theory and the geometric complexities of real-world columns. By accurately capturing the influence of cross-sectional shape, FRP properties, and concrete strength, it enables reliable, efficient, and physically grounded design and assessment of FRP-strengthened concrete structures, eliminating the need for multiple shape-specific formulations and reducing reliance on empirical approximations.

Statements & Declarations

Author contributions

Sajjad Shayanfar: Investigation, Formal analysis, Data curation, Software, Writing - Original Draft.

Meysam Ghasemi Naghibdehi: Project administration, Resources, Writing - Review & Editing.

Javad Shayanfar: Conceptualization, Methodology, Software, Writing - Review & Editing.

Funding

The authors received no financial support for the research, authorship, and/or publication of this article.

Data availability

The data presented in this study will be available on interested request from the corresponding author.

Declarations

The authors declare no conflict of interest.

References

[1] Isleem Haytham, F., Wang, Z., Wang, D., Smith Scott, T. Monotonic and Cyclic Axial Compressive Behavior of CFRP-Confined Rectangular RC Columns. Journal of Composites for Construction, 2018; 22: 04018023. doi:10.1061/(ASCE)CC.1943-5614.0000860.

[2] Nematzadeh, M., Mousavimehr, M., Shayanfar, J., Omidalizadeh, M. Eccentric compressive behavior of steel fiber-reinforced RC columns strengthened with CFRP wraps: Experimental investigation and analytical modeling. Engineering Structures, 2021; 226: 111389. doi:10.1016/j.engstruct.2020.111389.

[3] Liao, J., Zeng, J.-J., Zhuge, Y., Zheng, Y., Ma, G., Zhang, L. FRP-confined concrete columns with a stress reduction-recovery behavior: A state-of-the-art review, design recommendations and model assessments. Composite Structures, 2023; 321: 117313. doi:10.1016/j.compstruct.2023.117313.

[4] Wang, J., Xiao, H., Lu, L., Yang, J., Lu, S., Shayanfar, J. Axial stress-strain model for concrete in partially FRP wrapped reinforced concrete columns. Construction and Building Materials, 2024; 416: 135028. doi:10.1016/j.conbuildmat.2024.135028.

[5] Shayanfar, J., Barros Joaquim, A. O., Abedi, M., Rezazadeh, M. Unified Compressive Strength and Strain Ductility Models for Fully and Partially FRP-Confined Circular, Square, and Rectangular Concrete Columns. Journal of Composites for Construction, 2023; 27: 04023053. doi:10.1061/JCCOF2.CCENG-4336.

[6] Shayanfar, J., Barros, J. A. O., Pereira, J. P. C. A versatile model with a design framework for axially-loaded FRP-confined concrete with/without a stress reduction-recovery behavior. Construction and Building Materials, 2024; 448: 138097. doi:10.1016/j.conbuildmat.2024.138097.

[7] Shayanfar, J., Pereira, J. P. C., Barros, J. A. O. Passive confinement scenarios for strengthening fire-damaged concrete columns: Experimental and analytical research. Structures, 2025; 73: 108375. doi:10.1016/j.istruc.2025.108375.

[8] Shayanfar, J., Barros Joaquim, A. O. Design-Oriented Model of Unified Character to Determine Softening–Hardening Stress–Strain Behavior of FRP-Confined Concrete Columns of General Cross Section. Journal of Composites for Construction, 2024; 28: 04024059. doi:10.1061/JCCOF2.CCENG-4772.

[9] Shayanfar, J., Barros, J. A., Rezazadeh, M. Unified model for fully and partially FRP confined circular and square concrete columns subjected to axial compression. Engineering Structures, 2022; 251: 113355. doi:10.1016/j.engstruct.2021.113355.

[10] Shayanfar, J., Barros, J. A. O., Rezazadeh, M. Cross-sectional and confining system unification on peak compressive strength of FRP confined concrete. Structural Concrete, 2023; 24: 1531-1545. doi:10.1002/suco.202200105.

[11] Shayanfar, J., Barros, J. A. O., Rezazadeh, M., Kafshgarkolaei, H. J. Enhancing the performance of heat-damaged rectangular RC columns using prestressed FRP confinement. Construction and Building Materials, 2025; 501: 144346. doi:10.1016/j.conbuildmat.2025.144346.

[12] Ozbakkaloglu, T., Akin, E. Behavior of FRP-Confined Normal- and High-Strength Concrete under Cyclic Axial Compression. Journal of Composites for Construction, 2012; 16: 451-463. doi:10.1061/(ASCE)CC.1943-5614.0000273.

[13] Ozbakkaloglu, T. Axial Compressive Behavior of Square and Rectangular High-Strength Concrete-Filled FRP Tubes. Journal of Composites for Construction, 2013; 17: 151-161. doi:10.1061/(ASCE)CC.1943-5614.0000321.

[14] Wang, D. Y., Wang, Z. Y., Smith, S. T., Yu, T. Size effect on axial stress-strain behavior of CFRP-confined square concrete columns. Construction and Building Materials, 2016; 118: 116-126. doi:10.1016/j.conbuildmat.2016.04.158.

[15] Shayanfar, J., Bengar, H. A. A practical model for simulating nonlinear behaviour of FRP strengthened RC beam-column joints. Steel and Composite Structures, 2018; 27: 49-74. doi:10.12989/scs.2018.27.1.049.

[16] Shayanfar, J., Barros, J. A. O., Rezazadeh, M. Analytical model to predict axial stress-strain behavior of heat-damaged unreinforced concrete columns wrapped by FRP jacket. Engineering Structures, 2023; 289: 116244. doi:10.1016/j.engstruct.2023.116244.

[17] Shayanfar, J., Barros, J. A. O., Rezazadeh, M. Analysis-oriented model for partially FRP-and-steel-confined circular RC columns under compression. Engineering Structures, 2023; 276: 115330. doi:10.1016/j.engstruct.2022.115330.

[18] Li, P.-D., Zeng, Q., Jiang, J.-F. Stiffness-based stress–strain model of FRP-confined high-strength and ultra-high strength concrete column with various corner radii. Construction and Building Materials, 2023; 409: 133873. doi:10.1016/j.conbuildmat.2023.133873.

[19] Eid, R., Roy, N., Paultre, P. Normal- and High-Strength Concrete Circular Elements Wrapped with FRP Composites. Journal of Composites for Construction, 2009; 13: 113-124. doi:10.1061/(ASCE)1090-0268(2009)13:2(113).

[20] Wei, Y., Wu, Y.-F. Experimental Study of Concrete Columns with Localized Failure. Journal of Composites for Construction, 2016; 20: 04016032. doi:10.1061/(ASCE)CC.1943-5614.0000686.

[21] Fallah Pour, A., Nguyen, G. D., Vincent, T., Ozbakkaloglu, T. Investigation of the compressive behavior and failure modes of unconfined and FRP-confined concrete using digital image correlation. Composite Structures, 2020; 252: 112642. doi:10.1016/j.compstruct.2020.112642.

[22] Vincent, T., Ozbakkaloglu, T. Influence of concrete strength and confinement method on axial compressive behavior of FRP confined high- and ultra high-strength concrete. Composites Part B: Engineering, 2013; 50: 413-428. doi:10.1016/j.compositesb.2013.02.017.

[23] de Oliveira Diôgo, S., Raiz, V., Carrazedo, R. Experimental Study on Normal-Strength, High-Strength and Ultrahigh-Strength Concrete Confined by Carbon and Glass FRP Laminates. Journal of Composites for Construction, 2019; 23: 04018072. doi:10.1061/(ASCE)CC.1943-5614.0000912.

[24] Demir, U., Ispir, M., Sahinkaya, Y., Arslan, G., Ilki, A. Axial Behavior of Noncircular High-Performance Fiber-Reinforced Cementitious Composite Members Externally Jacketed by CFRP Sheets. Journal of Composites for Construction, 2019; 23: 04019022. doi:10.1061/(ASCE)CC.1943-5614.0000940.

[25] Shayanfar, J., Barros, J. A. O., Rezazadeh, M. Stress–strain model for FRP confined heat-damaged concrete columns. Fire Safety Journal, 2023; 136: 103748. doi:10.1016/j.firesaf.2023.103748.

[26] Shayanfar, J., Kafshgarkolaei, H. J., Barros, J. A. O., Rezazadeh, M. Unified strength model for FRP confined heat-damaged circular and square concrete columns. Composite Structures, 2023; 307: 116647. doi:10.1016/j.compstruct.2022.116647.

[27] Shayanfar, J., Barros Joaquim, A. O., Rezazadeh, M. Stress–Strain Model for FRP-Confined Circular Concrete Columns Developing Structural Softening Behavior. Journal of Composites for Construction, 2024; 28: 04023065. doi:10.1061/JCCOF2.CCENG-4364.

[28] Zeng, J.-J., Chen, J.-D., Liao, J., Chen, W.-J., Zhuge, Y., Liu, Y. Behavior of ultra-high performance concrete under true tri-axial compression. Construction and Building Materials, 2024; 411: 134450. doi:10.1016/j.conbuildmat.2023.134450.

[29] Wang, L.-M., Wu, Y.-F. Effect of corner radius on the performance of CFRP-confined square concrete columns: Test. Engineering Structures, 2008; 30: 493-505. doi:10.1016/j.engstruct.2007.04.016.

[30] Shan, B., Gui, F. C., Monti, G., Xiao, Y. Effectiveness of CFRP Confinement and Compressive Strength of Square Concrete Columns. Journal of Composites for Construction, 2019; 23: 04019043. doi:10.1061/(ASCE)CC.1943-5614.0000967.

[31] Han, Q., Yuan, W., Bai, Y., Du, X. Compressive behavior of large rupture strain (LRS) FRP-confined square concrete columns: experimental study and model evaluation. Materials and Structures, 2020; 53: 99. doi:10.1617/s11527-020-01534-4.

[32] Shayanfar, J., Rezazadeh, M., Barros, J., Ramezansefat, H. A New Dilation Model for FRP Fully/partially Confined Concrete Column Under Axial Loading. In: Proceedings of the 3rd RILEM Spring Convention and Conference (RSCC 2020); 2020 Mar 9-14; Cham, Switzerland. p. 435-446. doi:10.1007/978-3-030-76551-4_39.

[33] Shayanfar, J., Omidalizadeh, M., Nematzadeh, M. Analysis-oriented model for seismic assessment of RC jacket retrofitted columns. Steel and Composite Structures, 2020; 37: 371-390. doi:10.12989/scs.2020.37.3.371.

[34] Shayanfar, J., Barros, J. A. O., Rezazadeh, M. Generalized Analysis-oriented model of FRP confined concrete circular columns. Composite Structures, 2021; 270: 114026. doi:10.1016/j.compstruct.2021.114026.

[35] Cao, Y., Liu, Y., Li, X., Wu, Y. Axial stress strain behavior of FRP-confined rectangular rubber concrete columns with different aspect ratio. Engineering Structures, 2023; 297: 116987. doi:10.1016/j.engstruct.2023.116987.

[36] Abbasnia, R., Ziaadiny, H. Experimental investigation and strength modeling of CFRP-confined concrete rectangular prisms under axial monotonic compression. Materials and Structures, 2015; 48: 485-500. doi:10.1617/s11527-013-0198-y.

[37] Shayanfar, J., Bengar, H. A. Numerical model to simulate shear behaviour of RC joints and columns. Computers and Concrete, An International Journal, 2016; 18: 877-901. doi:10.12989/cac.2016.18.4.877.

[38] Shayanfar, J., Akbarzadeh Bengar, H. Nonlinear analysis of RC frames considering shear behaviour of members under varying axial load. Bulletin of Earthquake Engineering, 2017; 15: 2055-2078. doi:10.1007/s10518-016-0060-z.

[39] Cao, Y.-G., Jiang, C., Wu, Y.-F. Cross-Sectional Unification on the Stress-Strain Model of Concrete Subjected to High Passive Confinement by Fiber-Reinforced Polymer. Polymers, 2016; 8: 186. doi:10.3390/polym8050186.

[40] Guo, Y.-C., Xiao, S.-H., Luo, J.-W., Ye, Y.-Y., Zeng, J.-J. Confined Concrete in Fiber-Reinforced Polymer Partially Wrapped Square Columns: Axial Compressive Behavior and Strain Distributions by a Particle Image Velocimetry Sensing Technique. Sensors, 2018; 18: 4118. doi:10.3390/s18124118.

[41] Tariq, M., Khan, A., Shayanfar, J., Hanif, M. U., Ullah, A. A regression model for predicting the shear strength of RC knee joint subjected to opening and closing moment. Journal of Building Engineering, 2021; 41: 102727. doi:10.1016/j.jobe.2021.102727.

[42] Tariq, M., Khan, A., Ullah, A., Shayanfar, J., Niaz, M. Improved Shear Strength Prediction Model of Steel Fiber Reinforced Concrete Beams by Adopting Gene Expression Programming. Materials, 2022; 15: 3758. doi:10.3390/ma15113758.

[43] Onyelowe, K. C., Ebid, A. M., Mahdi, H. A., Soleymani, A., Jayabalan, J., Jahangir, H., Samui, P., Singh, R. P. Modeling the confined compressive strength of CFRP-jacketed noncircular concrete columns using artificial intelligence techniques. Cogent Engineering, 2022; 9: 2122156. doi:10.1080/23311916.2022.2122156.

[44] Abedi, M., Shayanfar, J., Al-Jabri, K. Infrastructure damage assessment via machine learning approaches: a systematic review. Asian Journal of Civil Engineering, 2023; 24: 3823-3852. doi:10.1007/s42107-023-00748-5.

[45] Shayanfar, J., Hemmati, A., Bengar, H. A. A simplified numerical model to simulate RC beam–column joints collapse. Bulletin of Earthquake Engineering, 2019; 17: 803-844. doi:10.1007/s10518-018-0472-z.

[46] Shayanfar, J., Barros, J. A. O., Rezazadeh, M. Design-oriented stress–strain model for RC columns with dual FRP- steel confinement mechanism. Composite Structures, 2024; 330: 117821. doi:10.1016/j.compstruct.2023.117821.

[47] Xie, J., Jia, C., Wang, Z. Data-driven machine-learning models for predicting non-uniform confinement effects of FRP-confined concrete. Structures, 2025; 74: 108555. doi:10.1016/j.istruc.2025.108555.

[48] Sadeghpour Haji, M., Niknam, R., Shayanfar, J. ANN-Based Modeling of Shear Behavior of Reinforced Concrete Columns under Constant Axial Loads. Civil Engineering and Applied Solutions, 2026; 2: 28-48. doi:10.22080/ceas.2025.30228.1050.

[49] Lam, L., Teng, J. G. Design-oriented stress–strain model for FRP-confined concrete. Construction and Building Materials, 2003; 17: 471-489. doi:10.1016/S0950-0618(03)00045-X.

[50] Teng, J. G., Jiang, T., Lam, L., Luo, Y. Z. Refinement of a Design-Oriented Stress–Strain Model for FRP-Confined Concrete. Journal of Composites for Construction, 2009; 13: 269-278. doi:10.1061/(ASCE)CC.1943-5614.0000012.

[51] Fallah Pour, A., Ozbakkaloglu, T., Vincent, T. Simplified design-oriented axial stress-strain model for FRP-confined normal- and high-strength concrete. Engineering Structures, 2018; 175: 501-516. doi:10.1016/j.engstruct.2018.07.099.

[52] International Federation for Structural Concrete. CEB-FIP: Externally applied FRP reinforcement for concrete structures. Lausanne (CH): FIB BULLETIN NO. 90; 2019.

[53] American Concrete Institute (ACI). ACI 440.2R-17: Guide for the design and construction of externally bonded FRP systems for strengthening concrete structures. Farmington Hills (MI): ACI; 2017.

[54] Shayanfar, J. Integrated modelling strategy for FRP-based confinement imposed to RC columns: From undamaged to post-fire damage (PhD Thesis). Braga (PT): University of Minho; 2024.

[55] Shayanfar, J., Akbarzadeh Bengar, H., Niroomandi, A. A proposed model for predicting nonlinear behavior of RC joints under seismic loads. Materials & Design, 2016; 95: 563-579. doi:10.1016/j.matdes.2016.01.098.

[56] Akbarzadeh Bengar, H., Abdollahtabar, M., Shayanfar, J. Predicting the Ductility of RC Beams Using Nonlinear Regression and ANN. Iranian Journal of Science and Technology, Transactions of Civil Engineering, 2016; 40: 297-310. doi:10.1007/s40996-016-0033-0.

[57] Bengar, H. A., Kiadehi, M. A., Shayanfar, J., Nazari, M. Effective flexural rigidities for RC beams and columns with steel fiber. Steel and Composite Structures, 2020; 34: 453-465. doi:10.12989/scs.2020.34.3.453.

[58] Abedi, M., Fangueiro, R., Correia, A. G., Shayanfar, J. Smart Geosynthetics and Prospects for Civil Infrastructure Monitoring: A Comprehensive and Critical Review. Sustainability, 2023; 15: 9258. doi:10.3390/su15129258.

[59] Abedi, M., Roshan, M. J., Gulisano, F., Shayanfar, J., Adresi, M., Fangueiro, R., Correia, A. G. An advanced cement-based geocomposite with autonomous sensing and heating capabilities for enhanced intelligent transportation infrastructure. Construction and Building Materials, 2024; 411: 134577. doi:10.1016/j.conbuildmat.2023.134577.

[60] Wei, Y.-Y., Wu, Y.-F. Unified stress–strain model of concrete for FRP-confined columns. Construction and Building Materials, 2012; 26: 381-392. doi:10.1016/j.conbuildmat.2011.06.037.